

Electrogenerated  $\text{IrO}_x$  Nanoparticles as Dissolved Redox Catalysts for Water Oxidation

Takaaki Nakagawa, Natalie S. Bjorge, and Royce W. Murray\*

Kenan Laboratories of Chemistry, University of North Carolina, Chapel Hill, North Carolina 27599-3290

Received July 28, 2009; E-mail: rwm@email.unc.edu

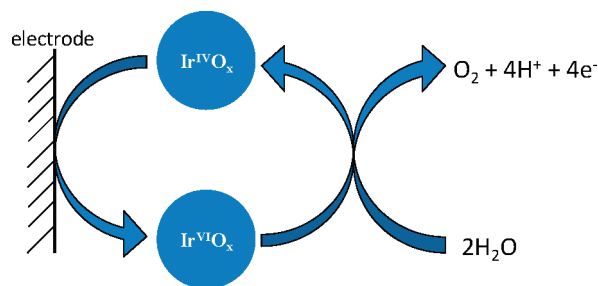
Using dissolved, freely diffusing molecules as electron transfer mediators is a common tactic in electrochemical redox catalysis.<sup>1</sup> Using dissolved, freely diffusing inorganic nanoparticles as electron transfer mediators has seldom been considered, however.<sup>2</sup> This paper reports mass transport-controlled  $\text{Ir}^{\text{V/IV}}$  and  $\text{Ir}^{\text{IV/III}}$  voltammetry in pH 13 solutions of  $\text{Ir}^{\text{IV}}\text{O}_x$  nanoparticles and the effectiveness of the  $\text{Ir}^{\text{V/IV}}$  step in the redox catalysis of the oxidation of water (Scheme 1). The  $\text{IrO}_x$  nanoparticles are very small ( $1.6 \pm 0.6$  nm dia., average 66 Ir/nanoparticle, see Supporting Information Figure S-1) and, being used in the same medium in which they are hydrolytically prepared,<sup>3</sup> are assumed to be capped solely by hydroxide. We show that their Ir sites are fully electroactive.

Rotated Pt disk voltammetry (RDE, Figure 1) of a pH 13 solution 2.5 mM in  $\text{Ir}^{\text{IV}}$  sites (38  $\mu\text{M}$  in nanoparticles, based on avg  $\text{IrO}_x$  nanoparticle size) shows three waves. Two, with  $E_{1/2} = 0.25$  and  $-0.62$  V, are assigned to  $\text{Ir}^{\text{V/IV}}$  and  $\text{Ir}^{\text{IV/III}}$  oxidation state changes in the nanoparticles and are mass transport controlled as shown by linear plots of limiting current vs  $\omega^{1/2}$  (inset) and concentration (see Figure S-2, inset). (RDE currents at intervening potentials are very small, meaning that the nanoparticles are initially in the  $\text{Ir}^{\text{IV}}$  state.) The currents steadily rising<sup>4a</sup> beyond the  $\text{Ir}^{\text{V/IV}}$  wave plateau (from ca.  $+0.45$  V) reflect electrochemical generation of  $\text{Ir}^{\text{VI}}$  states in the nanoparticles that act as redox catalysts for the  $\text{H}_2\text{O} \rightarrow \text{O}_2$  oxidation in the recycling of Ir states in Scheme 1. Currents in this  $4e^-$  catalytic wave, while proportional to nanoparticle concentration (Figure S-2, inset), are nearly independent of  $\omega$  (Figure 1 inset,  $\Delta$ ), which clearly signifies a rate-limiting reaction step in the nanoparticles' reaction(s) with water.<sup>4a</sup> Rotated ring-disk electrode (RRDE) results show that  $\text{Ir}^{\text{VI}}\text{O}_x$  nanoparticles electrogenerated at  $+1.0$  V (Figure 2) and at  $+0.55$  V (Figure S-3) produce  $\text{O}_2$  with 100% efficiency. (In the RRDE experiment,  $\text{O}_2$  produced by Scheme 1 near the disk is swept to the ring electrode and reduced in a  $2e^-$   $\text{O}_2 \rightarrow \text{H}_2\text{O}_2$  wave.) Based on the ring/disk current ratio, the observed collection efficiency  $N/2$  exactly matches the 11% expected from the RRDE geometry (see Figure 2 caption). That is, the redox catalysis reaction of Scheme 1 quantitatively converts oxidative charge delivered to the nanoparticles to the production of  $\text{O}_2$ .

This first electrochemical demonstration of water oxidation mediated by dissolved nanoparticles opens up the study of the water oxidation reaction (kinetics and mechanism) by manipulation of solution and transport parameters that are less readily controlled or ascertained for nanoparticles coated onto the electrode in an electrocatalytic film.

Indeed, we recently reported<sup>3</sup> the electrocatalysis of water oxidation by films of similarly prepared  $\text{IrO}_x$  nanoparticles that were electroflocculated onto electrodes, and which display catalytic properties similar to those we report here for the dissolved  $\text{IrO}_x$  nanoparticles (see Figure S-4). Thus, at 100% current efficiency and  $0.5 \text{ mA/cm}^2$ , film<sup>3</sup> and dissolved nanoparticles<sup>4b</sup> exhibit  $\eta = 0.29$  V. Both film and dissolved nanoparticle  $\eta$  results both surpass previous recent descriptions of electrocatalytic water oxidation (at

**Scheme 1.** Redox Catalysis of Water Oxidation with Dissolved, Diffusing  $\text{IrO}_x$  Nanoparticles



the same current density), by films on ITO electrodes (50–100 nm diameter citrate-stabilized  $\text{IrO}_2$  nanoparticles,  $\eta \approx 0.42$  V, pH 5.3),<sup>5</sup> and by films containing  $\text{Co}^{2+}$  and phosphate ( $\eta \approx 0.38$  V, pH 7).<sup>6</sup>

Another comparison of film and dissolved nanoparticles as catalysts is based on Ir site turnover frequency (TO, mol  $\text{O}_2/\text{Ir}$  sites/s). To make this comparison, conditions were selected that demonstrably (see Figure S-5) avoid electroflocculation<sup>3</sup> and consequent artifactual electrocatalysis by a nanoparticle film (e.g., the currents are due solely to diffusing nanoparticles.) In RDE voltammetry, the turnover (TO) frequency of iridium sites in dissolved  $\text{IrO}_x$  nanoparticles at 1.0 V and 300 rpm was estimated as  $8\text{--}11 \text{ s}^{-1}$  based on the ratio of currents at  $+1.0$  V (four electrons/Ir and Scheme 1 regeneration,  $\eta = 0.74$  V) to those at  $+0.4$  V (one electron,  $\text{Ir}^{\text{V/IV}}$  reaction, and no regeneration). The TO rate is independent of nanoparticle concentration (see Figure S-2) and is nearly the same as that ( $6 \text{ s}^{-1}$ ) measured<sup>3</sup> for films of electrofloc-

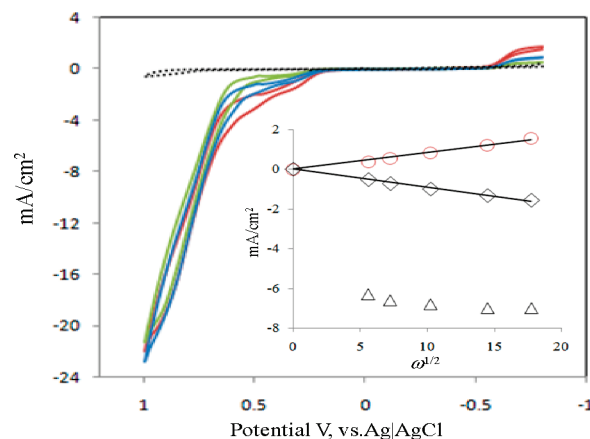


**Figure 1.** RDE (Pt disk) of deaerated pH 13  $\text{IrO}_x$  nanoparticle solution (2.5 mM in Ir sites) at electrode rotation rate  $\omega = 300$  (ocher), 1000 (blue), and 3000 rpm (red). The dashed black line is RDE in nanoparticle-free deaerated pH 13 solution at 300 rpm. Potential scan rate 20 mVs<sup>-1</sup>. Inset shows Levich plots (eq 2) at  $-0.8$  V (circle,  $\text{Ir}^{\text{IV/III}}$  wave),  $0.4$  V (diamond,  $\text{Ir}^{\text{V/IV}}$  wave) and  $0.7$  V (triangle, water oxidation by  $\text{Ir}^{\text{VI}}$ ).

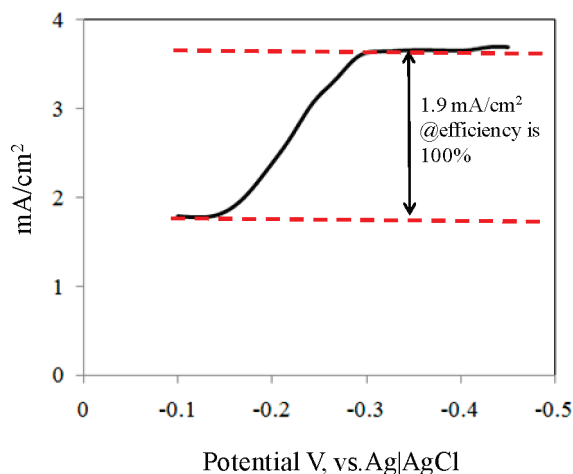


**Figure 2.** RRDE experiment. Oxygen reduction wave at Pt ring electrode (300 rpm) while Pt disk maintained at +1.0 V, in pH 13 deaerated IrO<sub>x</sub> nanoparticle solution ([Ir] = 2.5 mM). Potential scan rate 5 mV s<sup>-1</sup>. (During the scan, disk current decreased slightly (-17.1 to -16.3 mA cm<sup>-2</sup>). Ratio of ring to disk currents gives a collection efficiency ( $N/2$ ) of 11%, which accounting for disk (4e) and ring (2e) reactions and calibrated  $N$  of 22%, corresponds to 100% current efficiency for water oxidation to O<sub>2</sub>.

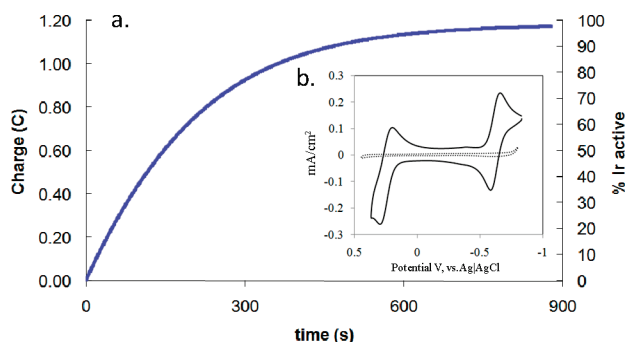


**Figure 3.** (a) Controlled potential coulometry on 5 mL of deaerated IrO<sub>2</sub> nanoparticle solution (containing 12.5 μmol Ir site) at pH 13 using platinum mesh electrode with stirring. The potential step is from -0.45 to -0.75 V. The current is reduction of Ir<sup>IV</sup> to Ir<sup>III</sup>. (b) CV of deaerated IrO<sub>2</sub> nanoparticle solution where [Ir] = 2.5 mM (black line) and control CV (dashed black line). pH 13, Pt disk electrode, scan rate 20 mV s<sup>-1</sup>.

culated IrO<sub>x</sub> nanoparticles. This result, that surface electrocatalysis and solution redox catalysis can show identical kinetics, is consonant with expectations<sup>1</sup> of chemically modified electrodes when the current is not electron or mass transport but reaction rate limited.

The Ir sites in the nanoparticles are exhaustively electroactive, as shown by controlled potential coulometry (Figure 3a). The collected charge for Ir<sup>IV</sup> → Ir<sup>III</sup> conversion was 96% of the Ir site concentration known to be present in the solution from the hydrolytic synthesis from IrCl<sub>6</sub><sup>2-</sup>. This complete reactivity contrasts with experiments on Ir oxide films<sup>7</sup> and 50 nm nanoparticle films,<sup>5</sup> where only a small fraction (3.7% and 16%, respectively) of the total Ir sites were electroactive. This seems clearly to be a nanoparticle size effect, wherein the very small electron and proton transport distances enable Ir site reactivity throughout the nanoparticle. The similarity of  $\eta$  and TO for electroflocculated and dissolved IrO<sub>x</sub> nanoparticles supports our previous<sup>3</sup> assumption of exhaustively electroactive Ir sites in the nanoparticles comprising the electroflocculated films.

The voltammetry of the dissolved IrO<sub>x</sub> nanoparticles at lower potentials is well-defined, as seen by RDE in Figure 1, inset and by CV in Figure 3b. The waves in the diffusion controlled CV, assigned to Ir<sup>V/IV</sup> and Ir<sup>IV/III</sup> reactions, are quasi-reversible ( $\Delta E_{\text{PEAK}} = 70$  mV) with formal potentials at  $E^{\circ} = -0.62$  and 0.25 V, agreeing with RDE observations (Figure 1). The nanoparticle diffusion coefficient was calculated from CV peak currents (see Figure S-6) and Levich plots (Figure 1, inset) using

$$i_{\text{PEAK}} = 2.69 \times 10^5 n^{3/2} A D^{1/2} \nu^{1/2} C_{\text{Ir}} \quad (1)$$

$$i_{\text{LIM}} = 0.62 n F A D^{2/3} \nu^{-1/6} \omega^{1/2} C_{\text{Ir}} \quad (2)$$

where  $n = 1$  and  $C_{\text{Ir}}$  = Ir site concentration, following previous multielectron transfer work<sup>8</sup> on dissolved redox polymers. The results,  $D = 3.3 \times 10^{-6}$  and  $4.0 \times 10^{-6}$  cm<sup>2</sup>/s, respectively, are consistent with the prediction,  $3.1(\pm 1.9) \times 10^{-6}$  cm<sup>2</sup>/s, of the Einstein–Stokes equation for a  $1.6(\pm 0.6)$  nm nanoparticle,

$$D = kT/6\pi\eta r \quad (3)$$

The diffusing IrO<sub>x</sub> nanoparticles seem well behaved as multi-electron electroactive species, which is a favorable portent for application of voltammetric mass transport principles to more deeply probe reactivities with water and other species.

In conclusion, we describe the electrochemical properties of  $1.6 \pm 0.6$  nm IrO<sub>x</sub> nanoparticles in aqueous solution. The nanoparticles' Ir<sup>IV/III</sup> and Ir<sup>V/IV</sup> reactions proceed at mass transport-controlled rates and are quasi-reversible. Bulk electrolysis reveals exhaustive electrochemical reactivity of the Ir nanoparticle sites, which we attribute to the small nanoparticle size allowing adequate electron and proton transport throughout. When driven to the Ir<sup>VI</sup> state, the nanoparticles oxidize water to O<sub>2</sub> at 100% current efficiency at overpotentials as small as 0.29 V.

**Acknowledgment.** This research was supported by grants from the NSF and Office of Naval Research, by a gift from Sony Corporation, and by equipment loaned from Pine Research Instrumentation.

**Supporting Information Available:** TEM, experimental details, and further RDE, RRDE, and CV results. This material is available free of charge via the Internet at <http://pubs.acs.org>.

## References

- (a) Savéant, J.-M. *Chem. Rev.* **2008**, *108* (7), 2348–2378. (b) Cracknell, J. A.; Vincent, K. A.; Armstrong, F. A. *Chem. Rev.* **2008**, *108* (7), 2439–2461.
- (a) Miller, D. S.; Bard, A. J.; McLendon, G.; Ferguson, J. *J. Am. Chem. Soc.* **1981**, *103*, 5336–5341. (b) Xiao, X.; Fan, F.-R. F.; Zhou, J.; Bard, A. J. *J. Am. Chem. Soc.* **2008**, *130*, 16669–16677.
- Nakagawa, T.; Beasley, C. A.; Murray, R. W. *J. Phys. Chem. C* **2009**, *113*, 12958–12961.
- (a) The interesting but vague current–potential features following the Ir<sup>V/IV</sup> current plateau, at the foot of the rise of water oxidation currents, and the linear Koutecky–Levich plots for the slight dependency on  $\omega$  of currents at +0.7 V in Figure 1 inset are undergoing further analysis. (b) The dissolved nanoparticle  $\eta$  value corresponds to the result at +0.55 V (Figure S-3) demonstrating O<sub>2</sub> production at 100% current efficiency.
- (a) Yagi, M.; Tomita, E.; Sakita, S.; Kuwabara, T.; Nagai, K. *J. Phys. Chem. B* **2005**, *109*, 21489–21491. (b) Kuwabara, T.; Tomita, E.; Sakita, S.; Hasegawa, D.; Sone, K.; Yagi, M. *J. Phys. Chem. C* **2008**, *112*, 3774–3779.
- (a) Kanan, M. W.; Nocera, D. G. *Science* **2008**, *321*, 1072. (b) Surendranath, Y.; Dincă, M.; Nocera, D. G. *J. Am. Chem. Soc.* **2009**, *131*, 2615–2620.
- Fierro, S.; Nagel, T.; Baltruschat, H.; Comminellis, T. *Electrochem. Solid-State Lett.* **2008**, *7*, E20–E23.
- Flanagan, J. B.; Margel, S.; Bard, A. J.; Anson, F. C. *J. Am. Chem. Soc.* **1978**, *100*, 4248–4253.

JA9063298